Ambiguities and Image Quality in Staggered SAR

Michelangelo Villano, Gerhard Krieger, Alberto Moreira
Microwaves and Radar Institute
German Aerospace Center (DLR)
Wessling, Germany
michelangelo.villano@dlr.de

***Abstract*—Staggered SAR is an innovative synthetic aperture radar (SAR) concept, where the pulse repetition interval (PRI) is continuously varied. This, together with digital beamforming (DBF) in elevation, allows high-resolution imaging of a wide continuous swath without the need for a long antenna with multiple azimuth apertures. As an additional benefit, the energy of range and azimuth ambiguities is spread over large areas: Ambiguities therefore appear in the image as a noise-like disturbance rather than localized artifacts. An analytical expression for the range-ambiguity-to-signal ratio (RASR) in staggered SAR is provided and a novel method for the estimation of the azimuth ambiguity-to-signal ratio (AASR) is proposed. A C-band design example based on a planar antenna is shown as well. The impact of staggered SAR operation on image quality is further assessed using highly oversampled F-SAR airborne data.**

***Index Terms*—Synthetic aperture radar (SAR), high-resolution wide-swath (HRWS) imaging, staggered SAR, ambiguities, range ambiguity-to-signal ratio (RASR), azimuth ambiguity-to-signal-ratio (AASR), Tandem-L.**

I. Introduction

Synthetic aperture radar (SAR) is a remote sensing technique, capable of providing high-resolution images independent of weather conditions and sunlight illumination [1]. This makes SAR very attractive for the systematic observation of dynamic processes on the Earth's surface. However, conventional SAR systems are limited, in that a wide swath can only be achieved at the expense of a degraded azimuth resolution, i.e., reducing the pulse repetition frequency (PRF) [2]. This limitation can be overcome by using systems with multiple receive apertures, displaced in along-track, which simultaneously acquire multiple samples for each transmitted pulse, but a very long antenna is required to map a wide swath. If a relatively short antenna with a single aperture in along-track is available, it is still possible to map a wide area: Multiple swaths can be, in fact, simultaneously imaged using digital beamforming (DBF) in elevation, but "blind ranges" are present between adjacent swaths, as the radar cannot receive while it is transmitting [3]. Most applications related to environmental monitoring and climate research, however, require a wide continuous swath, which also allows a more efficient coverage of large geographical areas.

Staggered SAR is an innovative concept, where the pulse repetition interval (PRI) is continuously varied, thus allowing the imaging of a wide continuous swath without the need for a long antenna with multiple apertures [4], [5]. If the PRI is continuously varied, even in a cyclical manner, i.e., repeating a sequence of PRIs, there will still be ranges, from which the echo is not received, because the radar is transmitting, but in general those ranges will be different for each transmitted pulse. If the overall synthetic aperture is considered, it turns out that at each slant range only some of the samples are missing. If missing samples are almost uniformly distributed across the swath, a relatively small percentage of pulses is missing at each slant range, data can be interpolated on a uniform grid, and azimuth compression can still be performed over a wide continuous swath. The staggered SAR concept is being considered for Tandem-L, which is a proposal for a polarimetric and interferometric satellite mission to monitor dynamic processes over the Earth's surface with unprecedented accuracy and resolution [6].

II. Range and Azimuth Ambiguities

Staggered SAR operation has significant effects on range and azimuth ambiguities. In a SAR system with constant PRI, during the acquisition of the raw data, the range ambiguous echoes of a scatterer are located at the same ranges along the whole synthetic aperture. This is due to the constant time distance to preceding and succeeding pulses and causes, after azimuth focusing, the presence of ghost targets in the SAR image, because the ambiguous energy is integrated along azimuth, even though the range migration is not fully matched, as for the scatterer. In a staggered SAR system, the range ambiguities are located at different ranges for different range lines, as the time distance to the preceding and succeeding pulses continuously varies. The ambiguous energy is therefore incoherently integrated and spread almost uniformly across the Doppler spectrum. If the mean PRF of the system PRF_{mean} is much larger than the processed Doppler bandwidth B_p, a significant amount of the ambiguous energy is filtered out during the SAR processing. Moreover, the residual ambiguous energy of a scatterer is spatially almost uniformly distributed over the whole synthetic aperture and over a slant range equal to the PRI span times half the speed of light. The same applies to nadir echoes, which result from the same phenomenon.

These peculiarities, as well as the specific sequence of PRIs, have to be taken into account for the evaluation of the range ambiguity-to-signal ratio (RASR). In particular, for a given sequence of PRIs, the RASR has to be evaluated for each of the M transmitted pulses of the sequence of PRIs. Due to the uniform distribution of the ambiguous energy, the RASR is then obtained for each slant range by averaging the RASR obtained for the M transmitted pulses

$$RASR \cong \frac{1}{M}\sum_{m=0}^{M-1}\left(\frac{\sum_{j=1}^{N_{A_m}}\frac{\sigma^0_{jm}\frac{B_p}{PRF_{mean}}\int_{f=-PRF_{mean}/2}^{PRF_{mean}/2}\left|G\left(\theta_{jm},f\right)\right|^2 df}{R^3_{jm}\sin\eta_{jm}}}{\frac{\sigma^0_{main}\int_{f=-B_p/2}^{B_p/2}\left|G\left(\theta_{main},f\right)\right|^2 df}{R^3_{main}\sin\eta_{main}}}\right) = \tag{1}$$

$$= \frac{\frac{1}{M}\sum_{m=0}^{M-1}\sum_{j=1}^{N_{A_m}}\frac{\sigma^0_{jm}\frac{B_p}{PRF_{mean}}\int_{f=-PRF_{mean}/2}^{PRF_{mean}/2}\left|G\left(\theta_{jm},f\right)\right|^2 df}{R^3_{jm}\sin\eta_{jm}}}{\frac{\sigma^0_{main}\int_{f=-B_p/2}^{B_p/2}\left|G\left(\theta_{main},f\right)\right|^2 df}{R^3_{main}\sin\eta_{main}}}$$

where σ^0 is the backscatter, $G(\theta,f)$ is the two-way two-dimensional (2D) antenna pattern (where θ is the elevation angle and f is the Doppler frequency), R is slant range, and η is the incidence angle. The subscript "main" refers to the desired return, the subscripts j, $j = 1..N_A$, to the N_A ambiguous (preceding and succeeding) returns and the subscripts m, $m = 0..M-1$, to the transmitted pulses of the sequence.

Fig. 1 (a) shows the RASR in dB for an L-band staggered SAR system with a 15 m reflector antenna, PRF_{mean} = 2700 Hz, and B_p = 780 Hz, evaluated using (1), while Fig.1 (b) shows the RASR for the same system operated with a constant PRF, equal to the mean PRF of the staggered SAR. The latter RASR is evaluated using the following formula, which accounts for the 2D antenna pattern

$$RASR \cong \frac{\sum_{j=1}^{N_A}\frac{\sigma^0_j\int_{f_D=-B_p/2}^{B_p/2}\left|G\left(\theta_j,f_D\right)\right|^2 df_D}{R^3_j\sin\eta_j}}{\frac{\sigma^0_{main}\int_{f_D=-B_p/2}^{B_p/2}\left|G\left(\theta_{main},f_D\right)\right|^2 df_D}{R^3_{main}\sin\eta_{main}}} \tag{2}$$

As apparent, the RASR is up to 5.5 dB better in the staggered SAR case, due to the aforementioned incoherent integration of the range ambiguous echoes.

As far as azimuth ambiguities are concerned, for a staggered SAR system it is not always straightforward to evaluate the azimuth ambiguity-to-signal ratio (AASR) using the azimuth antenna pattern as for a constant PRI SAR, because the resampling operation may change the shape of the azimuth spectrum of the signal. In order to assess the impact of azimuth ambiguities, therefore, the acquisition process and the signal processing has to be simulated, assuming that only a point-like scatterer is present in the scene. The focused data obtained from the simulation correspond to the 2D impulse response function (IRF) of the system. Fig. 2 shows the 2D IRF for a typical staggered SAR system, where azimuth ambiguities appear smeared.

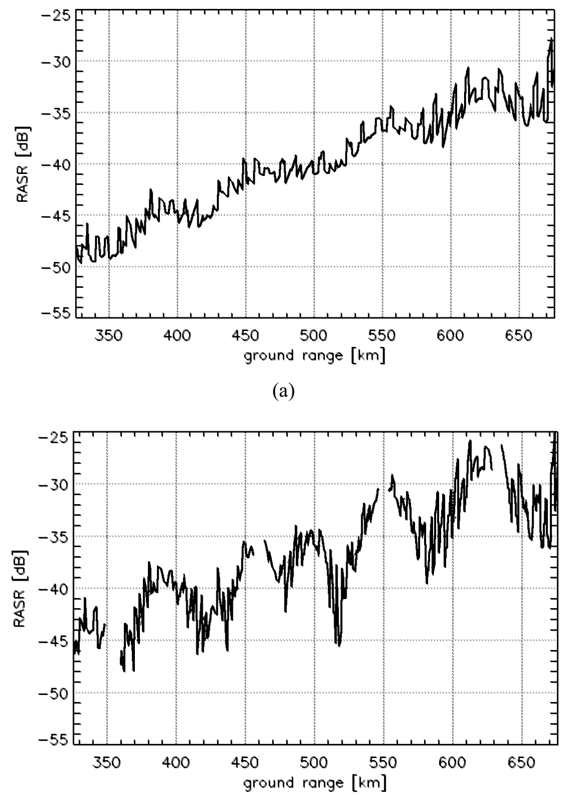

(b)

Fig. 1. *RASR* in dB. (a) Staggered SAR. (b) Constant *PRI* SAR with *PRF* equal to the mean *PRF* of the staggered SAR system.

Several performance parameters and in particular the integrated side lobe ratio (ISLR), defined as the ratio of the energy of all sidelobes to the mainlobe energy – can be then evaluated from the 2D IRF. Using the ISLR as a performance parameter, it has been shown in [4] that sequences of PRIs have to be preferred, for which two consecutive azimuth samples are never missed for all slant ranges of interest and the mean PRF is significantly larger than the Doppler bandwidth of the signal. This allows, in fact, the exploitation of the spectral properties of the azimuth signal within the resampling, using best linear unbiased (BLU) interpolation. The ISLR, however, is significantly influenced by the energy of the near sidelobes, so that a slight ISLR difference may result in a large AASR difference. Moreover, the ISLR strongly depends on the azimuth amplitude weighting, applied in the processing. In other words, it is not straightforward to establish a correspondence between ISLR and AASR, while the typical azimuth ambiguity requirement for SAR system is provided in terms of AASR and not ISLR.

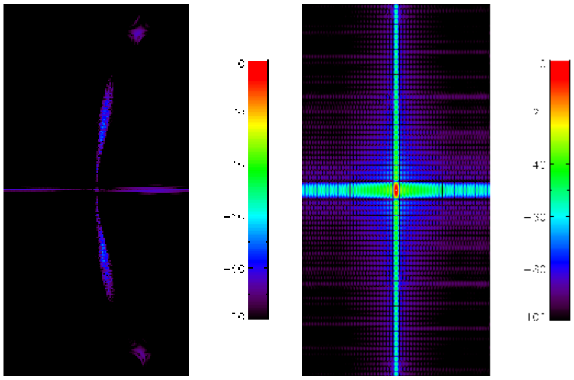

Fig. 2. 2D IRF (amplitude in dB) for a staggered SAR system (left) and zoom in the vicinity of the mainlobe (right). The horizontal and vertical axes represent slant range and azimuth, respectively.

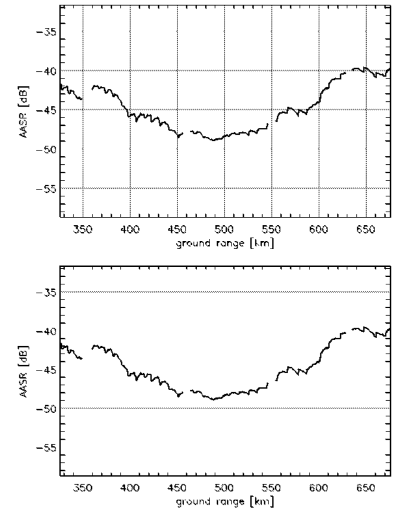

Fig. 3. Estimated AASR for a constant PRI SAR using the azimuth antenna pattern (top) and using the novel method based on the difference of the ISLRs (bottom).

In the following we propose a novel method to estimate the AASR in a staggered SAR system based on the 2D IRF. In particular, our AASR estimate is obtained as the difference of the attained ISLR and the ISLR of a constant PRI SAR with PRF equal to the mean PRF of the staggered SAR system, same values for the other system and processing parameters as the staggered SAR, and an azimuth antenna pattern equal to zero outside the processed Doppler bandwidth. Fig. 3 shows for a constant PRI SAR, which images multiple swaths, the estimated AASR using the azimuth antenna pattern and the novel method based on the difference of the ISLRs. As is apparent, the method based on the difference of the ISLRs provides a very accurate estimate of the AASR even for very low AASR levels.

There are two main reasons why 2D simulations have been preferred to one-dimensional (1D) (azimuth) simulations: First, 1D simulations do not provide the correct absolute levels of azimuth ambiguities for a point-like scatterer, as the defocusing of azimuth ambiguities is not accounted for; furthermore, possible effects related to the two-dimensional spatial distribution of the missing samples within the pulse extension would be neglected [7]-[10]. However, it can be observed that a 1D (azimuth) simulation still provides a good estimate for the AASR from the difference of the 1D (azimuth) ISLRs, while requiring a considerably smaller computational time. Fig. 4 shows the estimated AASR using the novel method based on the difference of the ISLRs for the aforementioned L-band staggered SAR system, evaluating the ISLRs from 1D and 2D IRFs. The difference of the two estimates is shown as well.

As apparent from the RASR and the AASR, evaluated as explained and displayed in Fig. 1 (a) and Fig. 4 (a), respectively, an L-band staggered SAR system with a 15 m reflector antenna allows imaging of a 350 km continuous swath with 10 m azimuth resolution and outstanding ambiguity performance (RASR and AASR better than -28 dB).

As shown in Fig. 5, the proposed AASR estimation technique can be also used to show how the AASR of a staggered SAR system varies for different interpolation methods, mean PRFs, processed Doppler bandwidths and mean duty cycles.

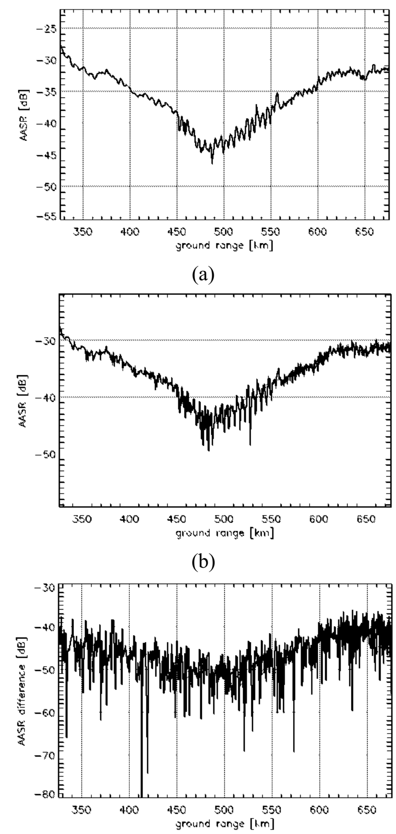

Fig. 4. Estimated AASR for a staggered SAR using the novel method based on the difference of the ISLRs. (a) Using 2D IRFs. (b) Using 1D IRFs. (c) Difference of the two estimates.

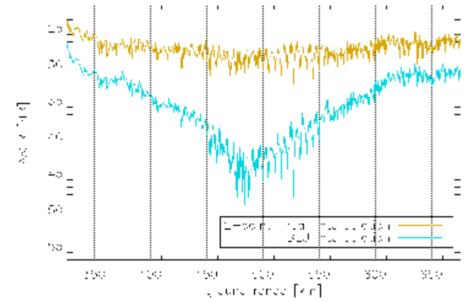

(a)

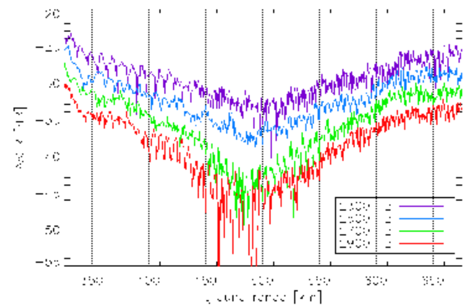

(b)

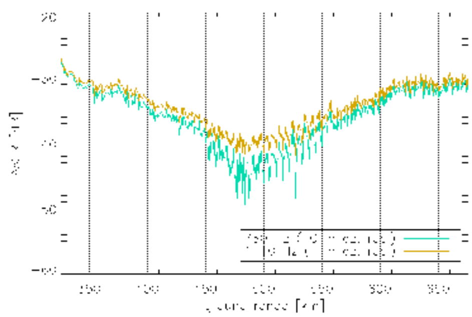

(c)

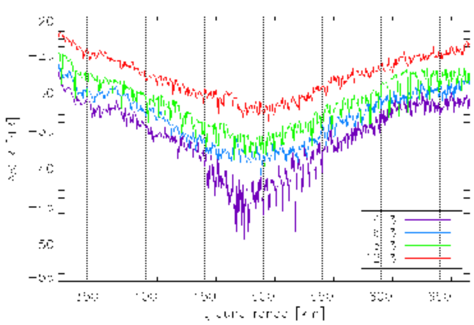

(d)

Fig. 5. Examples of applications of the proposed AASR estimation technique.
(a) AASR achieved for different staggered SAR resampling techniques, i.e., two-point linear interpolation and BLU interpolation.
(b) Dependence of the AASR on the mean PRF of the system.
(c) Dependence of the AASR on the processed Doppler bandwidth.
(d) Dependence of the AASR on the mean duty cycle.

III. C-Band Design Example

Using the analytical expression of the RASR provided in (1) and the proposed method for AASR estimation, the ambiguity performance of a C-band staggered SAR system based on a planar antenna have been evaluated. The system is assumed to be able to map a 400 km continuous ground swath in single- and dual-polarimetric modes and a 280 km continuous ground swath in fully-polarimetric mode, in both cases with a 5 m azimuth resolution. In particular, a 10 m × 2.6 m planar antenna with 36 elements in elevation has been considered. Fig. 6 shows the ambiguity performance for the single- and dual-polarimetric modes, which are outstanding (AASR better than -31 dB and RASR better than -36 dB), while Fig. 7 shows the performance for the fully-polarimetric mode, which are still compliant to typical ambiguity requirements (AASR better than -24.5 dB, RASR for the co-polarized channels better than -36 dB, RASR for the cross-polarized channels better than -24 dB).

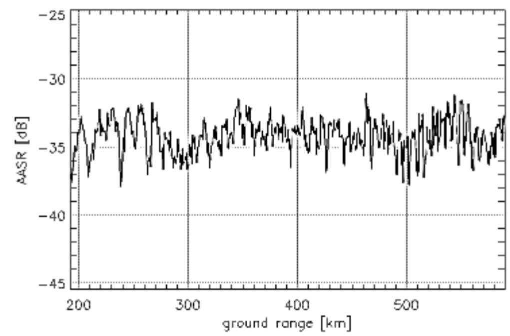

(a)

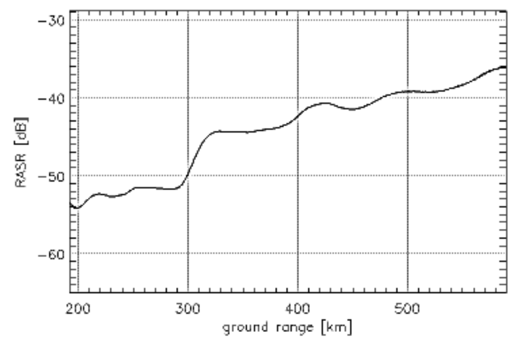

(b)

Fig. 6. Ambiguity performance for the C-band staggered SAR system based on a planar antenna for the single- and dual-polarimetric modes. (a) AASR. (b) RASR.

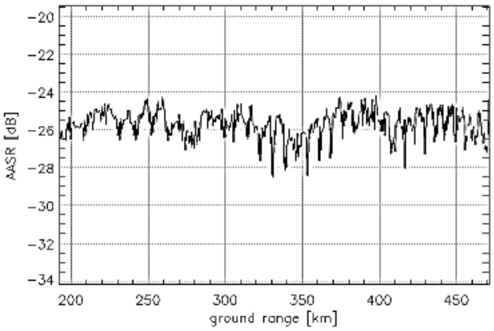

(a)

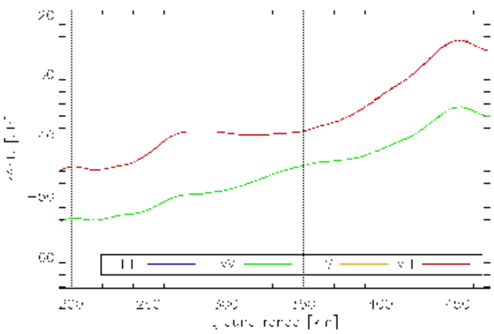

(b)

Fig. 7. Ambiguity performance for the C-band staggered SAR system based on a planar antenna for the fully-polarimetric mode. (a) AASR. (b) RASR.

IV. Image Quality Assessment using Oversampled Airborne Data

In order to better understand the implications of staggered SAR operation on image quality, airborne data with a PRF much larger than the Doppler bandwidth, i.e., highly oversampled in azimuth, have been also used. From the highly-oversampled raw data, it is possible to extract raw data as they would have been received by a staggered SAR system with arbitrary sequences of PRIs. These data can be then resampled to a uniform grid, allowing an assessment of the reconstruction error on raw data. Furthermore, conventional SAR processing can be performed and the image quality can be assessed for different oversampling rates, especially if several corner reflectors are present in the scene. For that reason, airborne data have been acquired by DLR's F-SAR sensor over the calibration test site of Kaufbeuren, Germany [11].

Fig. 8 shows the equivalent focused staggered SAR data, Fig. 9 shows the location of the twelve corner reflectors present in the scene, and Fig. 10 the simulated focused data assuming that only the twelve corner reflectors are present in the scene for different oversampling rates, while Table I shows for the aforementioned three cases the ISLR, evaluated on the simulated focused data, and the AASR, estimated according to the proposed novel method based on the difference of the ISLRs. In this case the ISLR of the reference constant PRI SAR with PRF equal to the mean PRF of the staggered SAR system, same values for the other system and processing parameters as the staggered SAR, and azimuth antenna pattern equal to zero outside the processed Doppler bandwidth is equal to -14.27 dB. The focused data obtained for a high oversampling rate do not show artifacts in correspondence of strong scatterers and are characterized by a higher image contrast. This is consistent with the AASR levels of Table I.

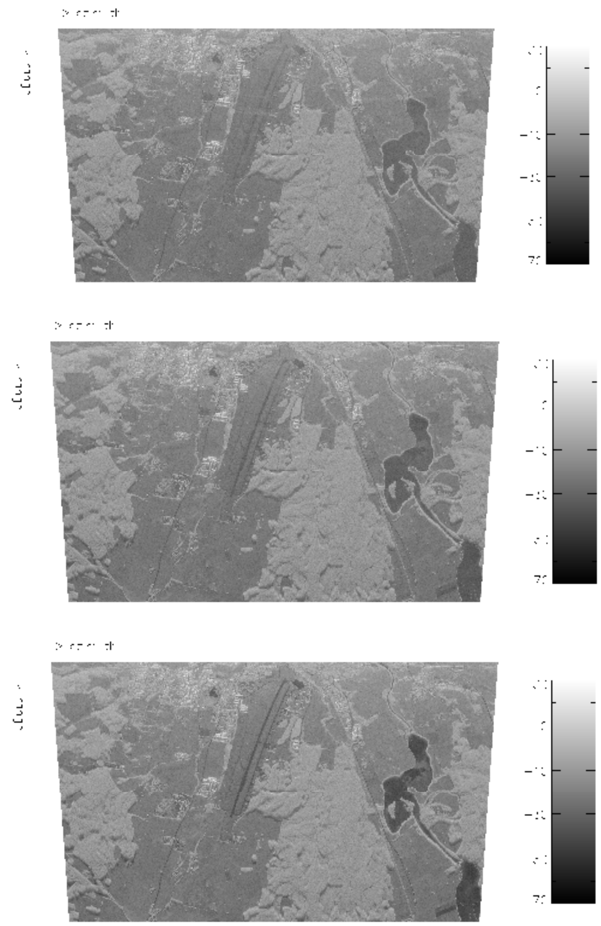

Fig. 8. Equivalent focused staggered SAR data acquired over Kaufbeuren for a low (top), medium (mid), and high (bottom) oversampling rate.

TABLE I. ISLR and AASR for the equivalent staggered SAR data set generated using highly oversampled F-SAR airborne data

Oversampling rate	ISLR	AASR
Low	-12.95 dB	-18.75 dB
Medium	-13.78 dB	-23.45 dB
High	-14.23 dB	-34.18 dB

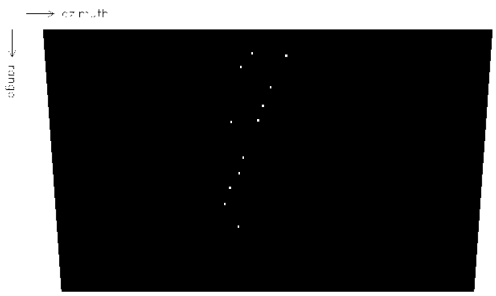

Fig. 9. Location of the twelve corner reflectors present in the scene.

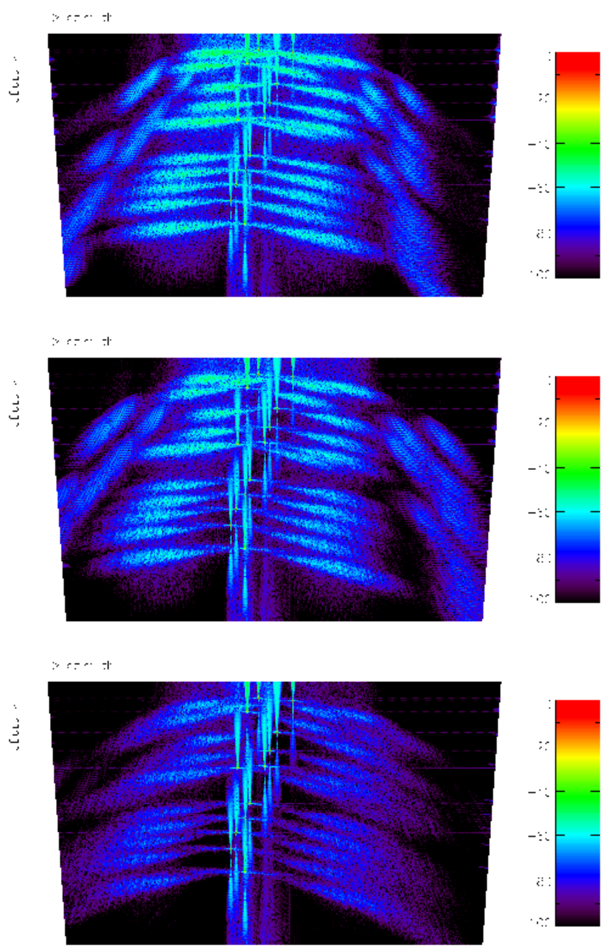

Fig. 10. Simulated focused data assuming that only the twelve corner reflectors are present in the scene for a low (top), medium (mid), and high (bottom) oversampling rate, corresponding to ISLR values of -12.95 dB, -13.78 dB and -14.23 dB, respectively.

V. Conclusion

New insights on range and azimuth ambiguities in staggered SAR have been presented, including an analytical expression for the RASR in staggered SAR and a novel method to estimate the AASR from the simulated IRF, which can be in principle applied to other systems as well. The image quality has been furthermore assessed using highly-oversampled F-SAR airborne data. Further analyses and experiments are planned in the near future.

References

[1] A. Moreira et al., “A Tutorial on Synthetic Aperture Radar,” *IEEE Geosci. Remote Sens. Mag.*, vol. 1, no. 1, 2013.

[2] A. Freeman, et al. "The “myth” of the minimum SAR antenna area constraint," *IEEE Transactions on Geoscience and Remote Sensing*, vol. 38, no .1, pp. 320-324, 2000.

[3] G. Krieger et al., “Advanced concepts for ultra-wide-swath SAR imaging,” *Proceedings of EUSAR*, Friedrichshafen, Germany, 2008.

[4] M. Villano, G. Krieger, A. Moreira, “Staggered SAR: High-Resolution Wide-Swath Imaging by Continuous PRI Variation,” *IEEE Trans. Geosci. Remote Sens.*, vol. 52, No. 7, pp. 4462-4479, 2014.

[5] M. Villano, G. Krieger, A. Moreira, “A Novel Processing Strategy for Staggered SAR,” *IEEE Geosci. Remote Sens. Lett.*, vol. 11, No. 11, pp. 1891-1895, 2014.

[6] A. Moreira et al., “Tandem-L: A Highly Innovative SAR Mission for Global Observation of Dynamic Processes on the Earth’s Surface,” *IEEE Geosci. Remote Sens. Mag.*, vol. 3, no. 2, 2015, in press.

[7] F. K. Li and W. T. K. Johnson, “Ambiguities in spaceborne synthetic aperture radar systems,” *IEEE Trans. Aerosp. Electron. Syst.*, vol. 19, no. 3, pp. 389–397, 1983.

[8] R. K. Raney and J. Prinz, “Reconsideration of azimuth ambiguities in SAR,” *IEEE Trans. Geosci. Remote Sens.*, vol. GE-25, No. 6, pp. 783-787, 1987.

[9] A. Moreira, “Suppressing the azimuth ambiguities in synthetic aperture radar images,” *IEEE Trans. Geosci. Remote Sens.*, vol. 31, no. 4, pp. 885–894, 1993.

[10] M. Villano and G. Krieger, “Spectral-Based Estimation of the Local Azimuth Ambiguity-to-Signal Ratio in SAR Images,” *IEEE Trans. Geosci. Remote Sens.*, vol. 52, no. 5, 2014.

[11] A. Reigber et al., “Very high-resolution airborne synthetic aperture radar imaging: Signal processing and application,” *Proceedings of the IEEE*, vol. 101, pp. 759–783, 2013.